Case Studies in Thermal Engineering 12 (2018) 374–380

Contents lists available at ScienceDirect

Case Studies in Thermal Engineering

journal homepage: www.elsevier.com/locate/csite

Case study of MHD blood flow in a porous medium with CNTS and thermal analysis

Asma Khalid[b], Ilyas Khan[a,*], Arshad Khan[c], Sharidan Shafie[d], I. Tlili[e]

[a] Faculty of Mathematics and Statistics, Ton Duc Thang University, Ho Chi Minh City, Vietnam
[b] Department of Mathematics, Sardar Bahadur Khan Women's University, Quetta 87300, Pakistan
[c] Institute of Business and Management Sciences, The University of Agriculture Peshawar, KPK, Pakistan.
[d] Department of Mathematical Sciences, Faculty of Science, Universiti Teknologi Malaysia, UTM, 81310 Skudai, Malaysia
[e] Energy and Thermal Systems Laboratory, National Engineering School of Monastir, Street Ibn El Jazzar, 5019 Monastir, Tunisia

ARTICLE INFO

Keywords:
Blood flow
Nanofluids
SWCNTs and MWCNTs
Thermal fluid
Exact solution

ABSTRACT

This articles deals with unsteady MHD free convection flow of blood with carbon nanotubes. The flow is over an oscillating vertical plate embedded in a porous medium. Both single-wall carbon nanotubes (SWCNTs) and multiple-wall carbon nanotubes (MWCNTs) are used with human blood as base fluid. The problem is modelled and then solved for exact solution using the Laplace transform technique. Expressions for velocity and temperature are determined and expressed in terms of complementary error functions. Results are plotted and discussed for embedded parameters. It is observed that velocity decreases with increasing CNTs volume fraction and an increase in CNTs volume fraction increases the blood temperature, which leads to an increase in the heat transfer rates. A validation of the present work is shown by comparing the current results with existing literature.

1. Introduction

The nanofluid model was first proposed by Choi [1], as a new class of heat transfer fluids that can be engineered by hanging metallic nanoparticles in conventional heat transfer fluids. The subsequent fluid recognized as nanofluid is probable to exhibit high thermal conductivities compared to those of currently used heat transfer fluids. The nanoparticles used in nanofluids are made of metals alumina, cupper, carbides, metal oxides, nitrides or non-metals (graphite, carbon nano-tubes) and usually water or ethylene glycol are used as base fluids [2–6]. CNTs as nanoparticles have held an essential role in the area of nanotechnology because of their unique electronic structural and mechanical characteristics. CNTs have extraordinary conductivity which helps them to form a network of conductive tubes. CNTs have also been consumed for thermal defense as thermal boundary materials. CNTs with high diffusion conductivity have attracted significantly important attention from researchers [7–9]. CNTs used in nanofluids are usually of two types, specifically single walls carbon nanotubes (SWCNTs) and multiple walls carbon nanotubes (MWCNTs). The width of CNTs ranges from 1 to 100 nm and lengths in micrometer. They have two hundred times power and five times resistance of steel, fifteen times thermal conductivity and 1000 times capability of copper [10–12]. Ding et al. [13] investigated the heat transfer behavior of CNT nanofluids flowing through a horizontal tube. They found important improvement of the convective heat transfer and observed that the improvement depends on solid volume fraction of CNTs and Reynolds number. Meyer et al. [14] presented the convective heat transfer enrichment of aqueous deferrals of MWCNTs flowing through a horizontal straight tube experimentally. The

* Corresponding author.
E-mail address: ilyaskhan@tdt.edu.vn (I. Khan).

https://doi.org/10.1016/j.csite.2018.04.004
Received 2 February 2018; Received in revised form 29 March 2018; Accepted 6 April 2018
Available online 23 April 2018

enhancement of thermal conductivity of ethylene glycol and synthetic engine oil in the presence of MWCNTs is reported by Liu et al. [15]. They found that CNTs-ethylene glycol suspensions have greater thermal conductivities as compare to ethylene glycol fluid without CNTs.

Wang et al. [16] experimentally investigated the heat transfer and pressure drop of nanofluids containing CNTs in a horizontal circular tube. They showed that the nanofluids at low concentration enhance the heat transfer with little extra penalty in pump power. An experimental study on the convective heat transfer characteristics of secondary refrigerant-based CNT nanofluids in a tubular heat exchanger given by Kumaresan et al. [17]. Khan et al. [18] reported numerically the flow and heat transfer of CNTs along a flat plate with Navier slip and uniform heat flux boundary conditions, they used SWCNTs and MWCNTs with three different base fluids. Haq et al. [19] studied water based flow in the presence of SWCNTs and MWCNTs, they examined a higher skin friction and Nusselt number for SWCNTs than MWCNTs. Kandasamy et al. [20] illustrated the impact of chemical reaction on Cu, Al_2O_3, and SWCNTs-nanofluid flow under the slip conditions numerically by using Runge-Kutta-Fehlberg Method with shooting technique and the impact of chemical reaction on SWCNTs, alumina and cupper nanoparticles on convective mass transfer in the presence of water base fluid by using numerical scheme also discussed by Kandasamy et al. [21]. Recently, exact solution of heat transfer enhancement in free convection flow of Maxwell nanofluids with SWCNTs and MWCNTs over a vertically static plate with constant wall temperature using Laplace transform technique presented by Aman et al. [22].

Amongst the non-Newtonian models, Casson model [24] is identified as the most preferred rheological model for describing human blood flow [25,26]. In this manuscript blood flow containing carbon nanotubes (CNTs) is scrutinized in the presence MHD and porosity. Blood is taken as base fluid with CNTs inside. Two types of CNTs (SWCNTs and MWCNTs) are taken. MHD and porosity effects are considered. The flow is considered over an oscillating plate. Laplace transform technique is used to obtain the analytical results. Numerical results for velocity and temperature are shown graphically and discussed in detail.

2. Problem formulation

The rheological equation of state for the Cauchy stress tensor of Casson fluid is written as, (see [16,24])

$$\tau_{ij} = \begin{cases} 2\left(\mu + \frac{p_y}{\sqrt{2\,\pi}}\right)e_{ij}, & \pi > \pi_c \\ 2\left(\mu + \frac{p_y}{\sqrt{2\,\pi_c}}\right)e_{ij}, & \pi < \pi_c \end{cases},$$

where $\pi = e_{ij}\, e_{ij}$ and e_{ij} is the $(i,\ j)^{ih}$ component of the deformation rate, π is the product of the component of deformation rate with itself, π_c is a critical value of this product based on the non-Newtonian model, μ is plastic dynamic viscosity of the non- Newtonian fluid and p_y is yield stress of fluid. Consider an incompressible unsteady flow of Casson-nanofluid containing CNTs of constant kinematic viscosity υ_{nf} occupying a semi-finite space $y > 0$. The plate is assumed to be electrically conducting with a uniform magnetic field B of strength B_0, applied in a direction perpendicular to the plate. The magnetic Reynolds number is assumed to be small enough to neglect the effect of applied magnetic field. The half space plate is embedded in a porous medium saturated with human blood based nanofluids containing SWCNTs and MWCNTs. The base fluid and CNTs are assumed to be in thermal equilibrium and no slip occurs between them. Initially, at time $t = 0$, both the fluid and the plate are at rest with constant temperature T_∞. In the meantime $t = 0^+$, the plate is subjected to sinusoidal oscillations so that, the $x-$ velocity at bounding wall is given by $V = UH(t)\cos(\omega t)$; U is the characteristics velocity, $H(t)$ is the unit step function, and ω is the frequency of oscillation of the plate. At the same time, the plate temperature is raised to T_w which is thereafter maintained constant [2,6]:

$$\rho_{nf}\frac{\partial u}{\partial t} = \mu_{nf}\left(1 + \frac{1}{\gamma}\right)\frac{\partial^2 u}{\partial \xi^2} - \left(\sigma_{nf}B_0^2 - \frac{\mu_{nf}}{k}\right)u + g(\rho\beta)_{nf}(T - T_\infty), \tag{1}$$

$$(\rho C_p)_{nf}\frac{\partial T}{\partial t} = k_{nf}\frac{\partial^2 T}{\partial \xi^2}, \tag{2}$$

together with initial and boundary conditions

$$t = 0{:}\ u(\xi,\ t) = 0,\ \ T(\xi,\ t) = T_\infty;\ \text{ for all } \xi > 0,\ t \geq 0{:}\ u = UH(t)\cos(\omega\, t),\ \ T = T_w;\ \xi = 0 t > 0{:}\ u(\xi,\ t) = 0,\ \ \ T(\xi,\ t) = 0;\ \xi \to \infty. \tag{3}$$

where u is the x-component of velocity, T is the temperature of Casson-nanofluid, $\gamma = \mu\sqrt{2\pi_c}/p_y$ is a Casson parameter, k_{nf} is the thermal conductivity of Casson-nanofluid, μ_{nf} is the dynamic viscosity of the Casson-nanofluid, ρ_{nf} is density of the Casson-nanofluid, $(\rho C_p)_{nf}$ is the heat capacitance of the Casson-nanofluid, β_{nf} is the thermal expansion coefficient of the Casson-nanofluid.

In this study, theoretical model proposed by Xue [9] based on Maxwell theory considering rotational elliptical nanotubes with very large axial ratio and compensating the effects of the space distribution on CNTs is used and given as

Table 1
Thermophysical properties of human blood and CNTs.

	$\rho(\mathrm{Kgm^{-3}})$	$C_p(JK\mathrm{g^{-1}K^{-1}})$	$k(\mathrm{Wm^{-1}K^{-1}})$	$\sigma(Sm^{-1})$	$\beta\times10^5(\mathrm{K^{-1}})$
Human blood	1053	3594	0.492	0.8	0.18
SWCNTs	2600	425	6600	10^6-10^7	27
MWCNTs	1600	796	3000	1.9×10^{-4}	44

$$\mu_{nf}=\frac{\mu_f}{(1-\phi)^{2.5}},\ \beta_{nf}=\frac{(1-\phi)(\rho\beta)_f+\phi(\rho\beta)_{\mathrm{CNTs}}}{\rho_{nf}},\ \rho_{nf}=(1-\phi)\rho_f+\phi\rho_{\mathrm{CNTs}},\ (\rho C_p)_{nf}=(1-\phi)(\rho C_p)_f+\phi(\rho C_p)_{\mathrm{CNTs}},\ \frac{\sigma_{nf}}{\sigma_f}$$
$$=\left\{1+\frac{3\left(\frac{\sigma_{\mathrm{CNTs}}}{\sigma_f}-1\right)\phi}{\left(\frac{\sigma_{\mathrm{CNTs}}}{\sigma_f}+2\right)-\phi\left(\frac{\sigma_{\mathrm{CNTs}}}{\sigma_f}-1\right)}\right\},\ \frac{k_{nf}}{k_f}=\frac{1-\phi+2\phi\frac{k_{\mathrm{CNTs}}}{k_{\mathrm{CNTs}}-k_f}\ln\frac{k_{\mathrm{CNTs}}+k_f}{2k_f}}{1-\phi+2\phi\frac{k_f}{k_{\mathrm{CNTs}}-k_f}\ln\frac{k_{\mathrm{CNTs}}+k_f}{2k_f}}, \tag{4}$$

where the subscripts f and CNTs are referred to fluid and carbon nanotubes to determine the thermal conductivity and the dimensionless heat transfer rates of nanofluid, where ϕ is the solid volume fraction of nanofluid. Thermophysical properties of the carrier fluid (human blood), SWCNTs and MWCNTs nanoparticles are given in Table 1.

The following dimensionless quantities are introduced

$$u^*=\frac{u}{U},\ \xi^*=\frac{\xi}{\sqrt{\upsilon t_0}},\ t^*=\frac{t}{t_0},\ \omega^*=\frac{\upsilon}{U^2}\omega,\ \theta=\frac{T-T_\infty}{T_w-T_\infty}, \tag{5}$$

into equations

$$\frac{\partial u}{\partial t}=\frac{1}{\phi_1}\left(1+\frac{1}{\gamma}\right)\frac{\partial^2u}{\partial\xi^2}-\left(\frac{M}{\phi_2}+\frac{\phi_1}{K}\right)u+Gr\phi_3\theta, \tag{6}$$

$$\frac{\partial\theta}{\partial t}=\frac{\lambda}{\mathrm{Pr}\phi_4}\frac{\partial^2\theta}{\partial\xi^2}, \tag{7}$$

with associated initial and boundary conditions

$$t=0:\ u(\xi,t)=0,\ \theta(\xi,t)=0\ ;\ \text{for all}\ \xi>0,\ t\geq0:\ u=H(t)\cos(\omega t),\ \theta=1;\ \xi=0,\ t>0:\ u(\xi,t)=0,\ \theta(\xi,t)=0;\ \xi\to\infty, \tag{8}$$

where

$$\mathrm{Pr}=\frac{\nu_f(\rho C_p)_f}{k_f},\ Gr=\frac{g\,\beta_f(T_w-T_\infty)\nu_f}{U^3},\ M=\frac{\sigma_f\nu_f{B_0}^2}{\rho_f\,U^2}\ \text{and}\ K=\frac{k_1U^2}{{\nu^2}_f},$$

are the Prandtl number, Grashof number, magnetic parameter and permeability parameter respectively. Besides that,

$$\lambda=\frac{k_{nf}}{k_f},\quad \phi_1=(1-\phi)^{2.5}\left\{(1-\phi)+\phi\frac{\rho_{\mathrm{CNTs}}}{\rho_f}\right\},\quad \phi_2=1+\frac{3\left(\frac{\sigma_{\mathrm{CNTs}}}{\sigma_f}-1\right)\phi}{\left(\frac{\sigma_{\mathrm{CNTs}}}{\sigma_f}+2\right)-\phi\left(\frac{\sigma_{\mathrm{CNTs}}}{\sigma_f}-1\right)}(1-\phi)+\phi\frac{\rho_{\mathrm{CNTs}}}{\rho_f},\ \phi_3$$
$$=\left\{\frac{(1-\phi)+\phi\frac{(\rho\beta)_{\mathrm{CNTs}}}{(\rho\beta)_f}}{(1-\phi)+\phi\frac{\rho_{\mathrm{CNTs}}}{\rho_f}}\right\},\quad \text{and}\quad \phi_4=\left\{(1-\phi)+\phi\frac{(\rho C_p)_{\mathrm{CNTs}}}{(\rho C_p)_f}\right\}$$

are functions depending upon the thermophysical properties of the base fluid and CNTs.

3. Solution of the problem

Applying Laplace transform, the following solutions for temperature and velocity are obtained:

$$\theta(\xi,t)=\mathrm{erfc}\left(\frac{\xi}{2}\sqrt{\frac{b_0}{t}}\right), \tag{9}$$

$$u(\xi,t)=u_m(\xi,t)+u_c(\xi,t), \tag{10}$$

$$u_m(\xi,t)=\frac{H(t)}{4}e^{-i\omega t}\left[e^{-\xi\sqrt{a_1(L-i\omega)}}\operatorname{erfc}\left(\frac{\xi}{2}\sqrt{\frac{a_1}{t}}-\sqrt{(L-i\omega)t}\right)+e^{\xi\sqrt{a_1(L-i\omega)}}\operatorname{erfc}\left(\frac{\xi}{2}\sqrt{\frac{a_1}{t}}+\sqrt{(L-i\omega)t}\right)\right]$$
$$+\frac{H(t)}{4}e^{i\omega t}\left[e^{-\xi\sqrt{a_1(L+i\omega)}}\operatorname{erfc}\left(\frac{\xi}{2}\sqrt{\frac{a_1}{t}}-\sqrt{(L+i\omega)t}\right)+e^{\xi\sqrt{a_1(L+i\omega)}}\operatorname{erfc}\left(\frac{\xi}{2}\sqrt{\frac{a_1}{t}}+\sqrt{(L+i\omega)t}\right)\right] \tag{11}$$

$$u_c(\xi,t)=b_1\left[\left(e^{-\xi\sqrt{a_1L}}\operatorname{erfc}\left(\frac{\xi}{2}\sqrt{\frac{a_1}{t}}\right)-\sqrt{Lt}\right)\left(\frac{t}{2}-\frac{\xi}{4}\sqrt{\frac{a_1}{L}}\right)+\left(e^{\xi\sqrt{a_1L}}\operatorname{erfc}\left(\frac{\xi}{2}\sqrt{\frac{a_1}{t}}\right)+\sqrt{Lt}\right)\left(\frac{t}{2}+\frac{\xi}{4}\sqrt{\frac{a_1}{L}}\right)\right]$$
$$-b_1\left[\left(t+\frac{b_0\xi^2}{2}\right)\operatorname{erfc}\left(\frac{\xi}{2}\sqrt{\frac{b_0}{t}}\right)-\xi\sqrt{b_0}\sqrt{\frac{t}{\pi}}e^{-\frac{b_0\xi^2}{4t}}\right], \tag{12}$$

where

$$a_0=\frac{\gamma}{1+\gamma},\quad a_1=a_0\phi_1,\quad b_0=\frac{\Pr\phi_3}{\lambda},\quad b_1=\frac{a_1Gr\phi_1\phi_2}{b_0-1}\quad\text{and}\quad L=\frac{M}{\phi_2}+\frac{\phi_1}{K}.$$

4. Special cases

4.1. Solution for newtonian fluids

By taking $\gamma\to\infty$ into Eq. (10), the corresponding solution for viscous fluid can be obtained as

$$u(\xi,t)=\frac{H(t)}{4}e^{-i\omega t}\left[e^{-\xi\sqrt{\phi_1(L-i\omega)}}\operatorname{erfc}\left(\frac{\xi}{2}\sqrt{\frac{\phi_1}{t}}-\sqrt{(L-i\omega)t}\right)+e^{\xi\sqrt{\phi_1(L-i\omega)}}\operatorname{erfc}\left(\frac{\xi}{2}\sqrt{\frac{\phi_1}{t}}+\sqrt{(L-i\omega)t}\right)\right]$$
$$+\frac{H(t)}{4}e^{i\omega t}\left[e^{-\xi\sqrt{\phi_1(L+i\omega)}}\operatorname{erfc}\left(\frac{\xi}{2}\sqrt{\frac{\phi_1}{t}}-\sqrt{(L+i\omega)t}\right)+e^{\xi\sqrt{\phi_1(L+i\omega)}}\operatorname{erfc}\left(\frac{\xi}{2}\sqrt{\frac{\phi_1}{t}}+\sqrt{(L+i\omega)t}\right)\right]$$
$$+b_1\left[\left(e^{-\xi\sqrt{\phi_1L}}\operatorname{erfc}\left(\frac{\xi}{2}\sqrt{\frac{\phi_1}{t}}\right)-\sqrt{Lt}\right)\left(\frac{t}{2}-\frac{\xi}{4}\sqrt{\frac{\phi_1}{L}}\right)+\left(e^{\xi\sqrt{\phi_1L}}\operatorname{erfc}\left(\frac{\xi}{2}\sqrt{\frac{\phi_1}{t}}\right)+\sqrt{Lt}\right)\left(\frac{t}{2}+\frac{\xi}{4}\sqrt{\frac{\phi_1}{L}}\right)\right]$$
$$-b_1\left[\left(t+\frac{b_0\xi^2}{2}\right)\operatorname{erfc}\left(\frac{\xi}{2}\sqrt{\frac{b_0}{t}}\right)-\xi\sqrt{b_0}\sqrt{\frac{t}{\pi}}e^{-\frac{b_0\xi^2}{4t}}\right].$$

4.2. Solution for Stokes' first problem

By taking $\omega\,t=0$ which corresponds to the impulsive motion of the plate, then Eq. (10) yield

$$u(\xi,t)=\frac{1}{2}\left[e^{-\xi\sqrt{a_1L}}\operatorname{erfc}\left(\frac{\xi}{2}\sqrt{\frac{a_1}{t}}-\sqrt{Lt}\right)+e^{\xi\sqrt{a_1L}}\operatorname{erfc}\left(\frac{\xi}{2}\sqrt{\frac{a_1}{t}}+\sqrt{Lt}\right)\right]+b_1\left[\begin{array}{l}\left(e^{-\xi\sqrt{a_1L}}\operatorname{erfc}\left(\frac{\xi}{2}\sqrt{\frac{a_1}{t}}\right)-\sqrt{Lt}\right)\left(\frac{t}{2}-\frac{\xi}{4}\sqrt{\frac{a_1}{L}}\right)\\+\left(e^{\xi\sqrt{a_1L}}\operatorname{erfc}\left(\frac{\xi}{2}\sqrt{\frac{a_1}{t}}\right)+\sqrt{Lt}\right)\left(\frac{t}{2}+\frac{\xi}{4}\sqrt{\frac{a_1}{L}}\right)\end{array}\right]$$
$$-b_1\left[\left(t+\frac{b_0\xi^2}{2}\right)\operatorname{erfc}\left(\frac{\xi}{2}\sqrt{\frac{b_0}{t}}\right)-\xi\sqrt{b_0}\sqrt{\frac{t}{\pi}}e^{-\frac{b_0\xi^2}{4t}}\right].$$

4.3. Solution without MHD and porosity effects

The temperature distribution is not effected by MHD and porous medium, as it results from Eq. (9). However, MHD and porosity have strong influence on velocity as it can be seen from the mechanical parts of Eq. (10). Thus in the absence of MHD ($M=0$) and porous medium ($K=0$), the equation become

$$u(\xi,t)=\frac{H(t)}{4}e^{-i\omega t}\left[e^{-\xi\sqrt{-a_1i\omega}}\operatorname{erfc}\left(\frac{\xi}{2}\sqrt{\frac{a_1}{t}}-\sqrt{-i\omega t}\right)+e^{\xi\sqrt{-a_1i\omega}}\operatorname{erfc}\left(\frac{\xi}{2}\sqrt{\frac{a_1}{t}}+\sqrt{-i\omega t}\right)\right]$$
$$+\frac{H(t)}{4}e^{i\omega t}\left[e^{-\xi\sqrt{a_1i\omega}}\operatorname{erfc}\left(\frac{\xi}{2}\sqrt{\frac{a_1}{t}}-\sqrt{i\omega t}\right)+e^{\xi\sqrt{a_1i\omega}}\operatorname{erfc}\left(\frac{\xi}{2}\sqrt{\frac{a_1}{t}}+\sqrt{i\omega t}\right)\right]$$
$$+b_1\left[\left(e^{-\xi\sqrt{a_1}}\operatorname{erfc}\left(\frac{\xi}{2}\sqrt{\frac{a_1}{t}}\right)\right)\left(\frac{t}{2}\right)+\left(e^{\xi\sqrt{a_1}}\operatorname{erfc}\left(\frac{\xi}{2}\sqrt{\frac{a_1}{t}}\right)\right)\left(\frac{t}{2}\right)\right]-b_1\left[\left(t+\frac{b_0\xi^2}{2}\right)\operatorname{erfc}\left(\frac{\xi}{2}\sqrt{\frac{b_0}{t}}\right)-\xi\sqrt{b_0}\sqrt{\frac{t}{\pi}}e^{-\frac{b_0\xi^2}{4t}}\right].$$

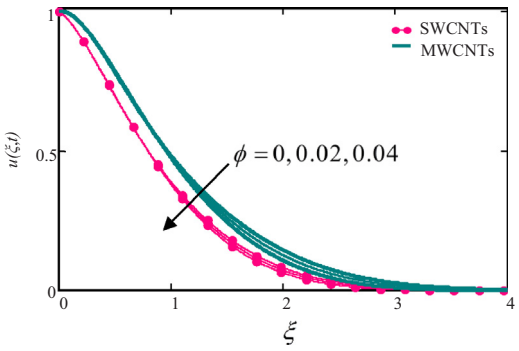

Fig. 1. Velocity profiles for different values of nanoparticle volume fraction ϕ in human blood-based nanofluid with SWCNTs & MWCNTs when $\gamma = 0.5$, Pr $= 21$, $Gr = 0.5$, $M = 0.2$, $K = 2$, $\omega t = 0$ & $t = 0.3$..

4.4. Solution in the absence of CNTs

Consider, pure Casson fluid without incorporating the CNTs, and by taking $\phi = 0$ and $\lambda = 0.0001$ into Eq. (10). Thus the resulting solution will be independent of the influence of CNTs and will be identical to those obtained by Khalid et al. [2], see Eq. (11). Hence, this confirms the accuracy of present results. This fact is also shown graphically in Fig. 6.

4.5. Solution for newtonian fluid with the absence of CNTs

By taking $\gamma \to \infty$, $\phi = 0$ and $\lambda = 0.0001$ into Eq. (10), the corresponding solution for viscous fluid will be independent of the effect of CNTs and the present result is in good agreement with the previous result found by Chaudhary and Jain [23], see equation (19).

5. Results and discussion

In the numerical computations the properties of blood and SWCNTs and MWCNTs are used from Table 1. The Prandtl number of blood is taken as Pr $= 25$. Fig. 1 depicts the effects of volume fraction ϕ $(0 \leq \phi \leq 0.04)$ on the velocity profiles for human blood-based nanofluid with SWCNTs and MWCNTs. It is observed that for both SWCNTs and MWCNTs, as the ϕ increases, the velocity of the nanofluid decreases. It is also noted that changes in ϕ indicates to changes in temperature and then velocity which in turn displays the significance of nanofluids in the procedures comprising heating and cooling. The influence blood parameter γ on velocity profiles is illustrated in Fig. 2. It is observed that for increasing the value of γ the velocity profile decreases for SWCNTs as well as for MWCNTs. Physically it is because of plasticity of blood, when γ decreases the plasticity of fluid increases which causes the deceleration in velocity.

Fig. 3 reveals the effect of the magnetic parameter M on velocity profiles. The velocity profiles decrease (for both types of CNTs) with increasing values M leading to a reduction in the velocity boundary layer thickness. Physically, the Lorentz force which opposes the motion occurs due to the applied transverse magnetic field, and is responsible for reducing the fluid velocity. In Fig. 4, the profiles of velocity for different vales of permeability parameter K are plotted. It is observed that for large values of K, velocity and boundary layer thickness increase which explains the physical situation that as K increases, the resistance of the porous medium is lowered which increases the momentum development of the flow regime ultimately enhances the velocity field for both SWCNTs and MWCNTs.

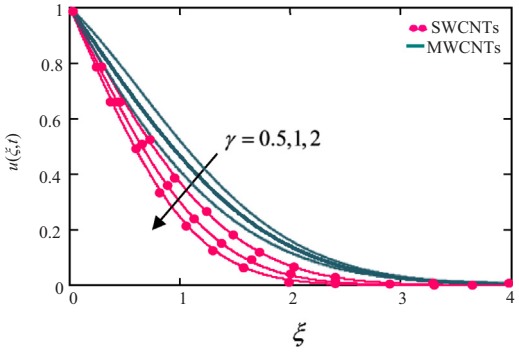

Fig. 2. Velocity profiles for different values of γ in human blood-based nanofluid with SWCNTs & MWCNTs when Pr $= 21$, $Gr = 0.5$, $M = 0.2$, $K = 2$, $\omega t = 0$ & $t = 0.3$..

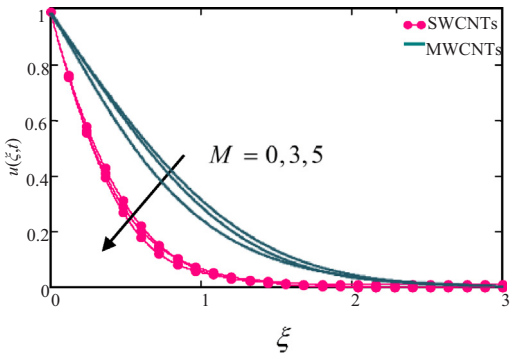

Fig. 3. Velocity profiles for different values of M in human blood-based nanofluid with SWCNTs & MWCNTs when $\gamma = 0.5$, Pr = 21, $Gr = 0.5$, $K = 0.2$, $\omega t = 0$ & $t = 0.3$..

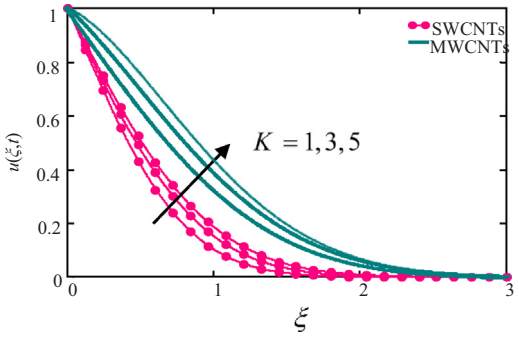

Fig. 4. Velocity profiles for different values of K in human blood-based nanofluid with SWCNTs & MWCNTs when $\gamma = 0.5$, Pr = 21, $Gr = 0.5$, $M = 0.5$, $\omega t = 0$ & $t = 0.3$..

Fig. 5 displays the influence of ϕ on temperature profiles. The fluid temperature increases with increasing values of ϕ for SWCNTs as well as for MWCNTs. Substantially, this is due to the cause that an rise in ϕ indications to an rise in the thermal conductivity of the CNTs nanofluid and hereafter the viscosity of the thermal boundary layer rises. Aman et al. [22] observed the same flow patterns.

For verification, present results are matched with those obtained by Khalid et al. [2] and Chaudhary and Jain [23]. This comparison is plotted in Fig. 6. It is found that present results without incorporating the CNTs, and by taking $\phi = 0$ and $\lambda = 0.0001$ are duplicate to those obtained by Khalid et al. [2], see Eq. (11) and when $\gamma \to \infty$, $\phi = 0$ and $\lambda = 0.0001$, the present results found in good agreement with previous published results obtained by Chaudhary and Jain [23], see equation (19). Hence, this approves the correctness of obtained results.

6. Final remarks

The final remarks are concluding from this study:

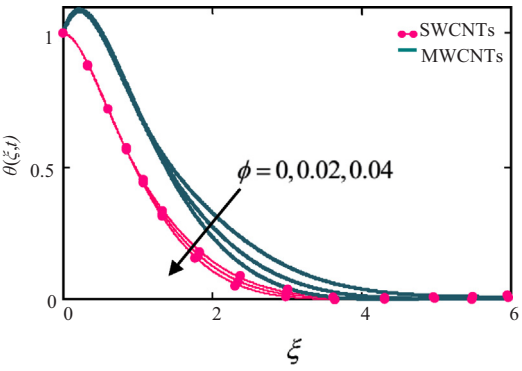

Fig. 5. Effects of nanoparticle volume fraction ϕ on the temperature of human blood-based with SWCNTs & MWCNTs nanofluid, when Pr = 21, $Gr = 0.5$..

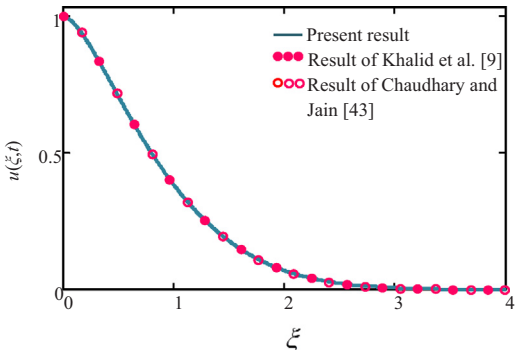

Fig. 6. Comparison of the present result without CNTs, see Eq. (10) when $\phi = 0$ and $\lambda = 0.0001$ with that obtained by Khalid et al. [2] see Eq. (11) and when $\gamma \to \infty$, $\phi = 0$ and $\lambda = 0.0001$ with Chaudhary and Jain [23], see equation (19).

- Velocity of Casson-nanofluid decreases with increasing CNTs volume fraction, Prandtl number and magnetic parameter, whereas increases with an increase in Grashof number and permeability parameter.
- An increase in CNTs volume fraction increases the Casson-nanofluid temperature, which leads to an increase in the heat transfer rates.
- SWCNTs and MWCNTs have the same effects on velocity and temperature profiles for Casson-nanofluid flow.
- Human blood as a base fluid used first time to obtain the exact solutions for Casson-nanofluids.
- Solution (10) is found in excellent agreement with those achieved by Khalid et al. [2] and Chaudhary and Jain [23].

References

[1] S. Choi, Enhancing thermal conductivity of fluids with nanoparticles, ASME Publ.-Fed. 231 (1995) 99–106.
[2] A. Khalid, I. Khan, A. Khan, S. Shafie, Unsteady MHD free convection flow of Casson fluids past over an oscillating vertical plate embedded in a porous medium, Eng. Sci. Technol.: Int. J. 18 (2015) 309–317.
[3] J. Buongiorno, Convective transport in nanofluids, ASME J. Heat Transf. 128 (2006) 240–250.
[4] J. Buongiorno, D.C. Venerus, N. Prabhat, et al., A benchmark study on the thermal conductivity of nanofluids, J. Appl. Phys. 106 (9) (2009) (Article ID 094312).
[5] M.Y. Malik, M. Naseer, S. Nadeem, Abdul Rehman, The boundary layer flow of Casson nanofluid over a vertical exponentially stretching cylinder, Appl. Nanosci. 4 (2014) 869–873.
[6] M. Mustafa, J.A. Khan, Model for flow of Casson nanofluid past a non-linearly stretching sheet considering magnetic field effects, AIP Adv. 5 (2015) 077148, http://dx.doi.org/10.1063/1.4927449.
[7] J. Choi, Y. Zhang, Properties and Applications of Single-, Double- and Multi-Walled Carbon Nanotubes, Aldrich Materials Science, Sigma-Aldrich Co. LLC, 1995.
[8] Y.J. Kim, T.S. Shin, H. Do Choi, J.H. Kwon, Y.C. Chung, H.G. Yoon, Electrical conductivity of chemically modified multiwalled carbon nanotube/epoxy composites, Carbon 43 (2005) 23–30.
[9] Q. Xue, Model for thermal conductivity of carbon nanotube based composites, Phys. B Condens. Matter 368 (2005) 302–307.
[10] X. Ma, F. Su, J. Chen, T. Bai, Z. Han, Enhancement of bubble absorption process using a CNTs-ammonia binary nanofluid, Int. Commun. Heat Mass 36 (2009) 657–660.
[11] Y. Xuan, Conception for enhanced mass transport in binary nanofluids, Heat Mass Transf. 46 (2009) 277–279.
[12] V. Prajapati, P.K. Sharma, A. Banik, Carbon nanotubes and its applications, Int. J. Pharm. Sci. Res. 2 (5) (2011) 1099–1107.
[13] Y. Ding, H. Alias, D. Wen, R.A. Williams, Heat transfer of aqueous suspensions of carbon nanotubes (CNT nanofluids), Int. J. Heat Mass Transf. 49 (1–2) (2006) 240–250.
[14] J. Meyer, T. McKrell, K. Grote, The influence of multi-walled carbon nanotubes on single-phase heat transfer and pressure drop characteristics in the transitional flow regime of smooth tubes, Int. J. Heat Mass Transf. 58 (1–2) (2013) 597–609.
[15] M.S. Liu, M.C.C. Lin, H. I-Te, C.C. Wang, Enhancement of thermal conductivity with carbon nanotube for nanofluids, Int. Commun. Heat Mass Transf. 32 (2005) 1202–1210.
[16] J. Wang, J. Zhu, X. Zhang, Y. Chen, Heat transfer and pressure drop of nanofluids containing carbon nanotubes in laminar flows, Exp. Therm. Fluid Sci. 44 (2013) 716–721.
[17] V. Kumaresan, R. Velraj, S.K. Das, Convective heat transfer characteristics of secondary refrigerant based CNT nanofluids in a tubular heat exchanger, Int. J. Refrig. 35 (8) (2012) 2287–2296.
[18] W.A. Khan, Z.H. Khan, M. Rahi, Fluid flow and heat transfer of carbon nanotubes along a flat plate with Navier slip boundary, Appl. Nanosci. 4 (2014) 633–641.
[19] R.U. Haq, S. Nadeem, Z.H. Khan, N.F.M. Noor, Convective heat transfer in MHD slip flow over a stretching surface in the presence of carbon nanotubes, Phys. B Condens. Matter 457 (2015) 40–47.
[20] R. Kandasamy, R. Mohamad, M. Ismoen, Impact of chemical reaction on Cu, Al_2O_3, and SWCNTs-nanofluid flow under slip conditions, Eng. Sci. Technol. Int. J. (2015).
[21] R. Kandasamy, I. Muhaimin, R. Mohammad, Single walled carbon nanotubes on MHD unsteady flow over a porous wedge with thermal radiation with variable stream conditions, Alex. Eng. J. 55 (2016) 275–285.
[22] S. Aman, I. Khan, Z. Ismail, M.Z. Salleh, Q.M. Al-Mdalla, Heat transfer enhancement in free convection flow of CNTs Maxwell nanofluids with four different types of molecular liquid, Sci. Rep. 7 (2017) 2445, http://dx.doi.org/10.1038/s41598-017-01358-3.
[23] R.C. Chaudhary, A. Jain, Combined heat and mass transfer effects on MHD free convection flow past an oscillating plate embedded in porous medium, Rom. J. Phys. 52 (2007) 505–524 (Bucharest).
[24] N. Casson, A flow equation for the pigment oil suspensions of the printing ink type, in: Rheology of Disperse Systems, pp. 84-102, Pergamon, NewYork, NY, USA, 1959.
[25] Swati Mukhopadhyay, Krishnendu Bhattacharyya, Tasawar Hayat, Exact solutions for the flow of Casson fluid over a stretching surface with transpiration and heat transfer effects, Chin. Phys. B 22 (11) (2013) 114701.
[26] Swati Mukhopadhyay, Casson fluid flow and heat transfer over a nonlinearly stretching surface, Chin. Phys. B 22 (7) (2013) 074701.